Available online at www.sciencedirect.com

ScienceDirect

Geochimica et Cosmochimica Acta 126 (2014) 411–421

Geochimica et Cosmochimica Acta

www.elsevier.com/locate/gca

Siderite 'clumped' isotope thermometry: A new paleoclimate proxy for humid continental environments

Alvaro Fernandez *, Jianwu Tang, Brad E. Rosenheim

Tulane University, Department of Earth and Environmental Science, 6823 St. Charles Avenue, New Orleans, LA, USA

Received 19 July 2013; accepted in revised form 6 November 2013; available online 21 November 2013

Abstract

Clumped isotope measurements can be used to exploit the paleoclimatic potential of pedogenic siderite ($FeCO_3$); however, the applicability of this method is held back by the lack of clumped isotope calibrations of mineralogies other than calcite and aragonite. Here we present an inorganic calibration of siderites grown in the laboratory between 21 and 51 °C. Linear regression of Δ_{47} values and temperature ($10^6/T^2$, K) yields the following relationship ($r^2 = 0.997$):

$$\Delta_{47\text{-RF}} = \frac{(0.0356 \pm 0.0018) \times 10^6}{T^2} + (0.172 \pm 0.019)$$

We demonstrate that this calibration is indistinguishable from calcite at current levels of analytical precision. Our observations suggest that there is likely no large systematic bias in the clumped isotope acid fractionation factors between the two different carbonate minerals. We also present clumped isotope measurements of a natural siderite collected from Holocene sediments of the Mississippi River Delta. We find that siderites record warm season marsh water temperatures instead of mean annual temperatures as it has long been presumed. This finding has important implications for the accuracy of siderite stable isotope and clumped isotope based climate reconstructions.

1. INTRODUCTION

Siderite ($FeCO_3$) has the potential to become an important archive of paleoclimate in humid continental environments because it forms in poorly drained/anoxic wetland soils where pedogenic calcite is not typically found (Ludvigson et al., 1998, 2013; Sheldon and Tabor, 2009). The oxygen isotope composition of siderite can be used to solve the carbonate-water isotope exchange paleothermometer equation for temperatures of mineral precipitation or for the $\delta^{18}O$ values of soil waters during mineral formation (White et al., 2001; Ufnar et al., 2004; Suarez et al., 2011). The paleothermometer equation, however, is a function of two independent variables (temperature and the $\delta^{18}O$ of the fluids from which the mineral forms) and one of them must be known independently to determine the other.

Like other carbonate minerals, $\delta^{18}O$ values of siderites can only be used when there are independent constraints on either the formation temperature or the $\delta^{18}O$ value of coexisting fluids. White et al. (2001) used the oxygen isotope composition of middle Cretaceous pedogenic siderites along with paleotemperature estimates from a general circulation model (GMC) to estimate meteoric water $\delta^{18}O$ values and, ultimately, arrive at an estimate for precipitation rate. While this approach is useful when direct observations are lacking, it uses model data in place of recorded observations. For instance, Suarez et al. (2011) used the pedogenic siderite data of Ufnar et al. (2002) along with new proxy data in a mass balance model to quantify the mid-Cretaceous hydrologic cycle. They found that the estimated rainfall rates depend strongly on the chosen Cretaceous

* Corresponding author. Tel.: +1 5048624922.
E-mail address: afernan4@tulane.edu (A. Fernandez).

0016-7037/$ - see front matter © 2013 Elsevier Ltd. All rights reserved.
http://dx.doi.org/10.1016/j.gca.2013.11.006

temperature reconstruction. Even if accurate, GCM temperature estimates may not be adequately precise, both temporally and spatially, to reflect local conditions during the time of mineral precipitation. For instance, solar heating can result in soil temperatures hotter than local air temperature (Passey et al., 2010; Quade et al., 2013); and, more importantly, it is not clear whether siderites record mean annual air temperatures (MAAT) or seasonally biased soil temperatures like pedogenic calcites (Breecker et al., 2009; Passey et al., 2010; Peters et al., 2013; Quade et al., 2013). This must be known before we can confidently interpret paleotemperature estimates from this archive.

Recent work has demonstrated that the carbonate clumped isotope paleothermometer is useful for solving both temperature and $\delta^{18}O_w$ problems simultaneously because it provides temperature estimates that are independent of fluid isotopic compositions (e.g., Ghosh et al., 2006; Schauble et al., 2006; Eiler, 2011). This effectively reduces the paleothermometer equation to one variable that can be reliably measured in the laboratory. The clumped isotope proxy exploits the observation that in the carbonate lattice the rare, heavier carbon and oxygen isotopes preferentially bond to each other with decreasing temperature. Isotopic 'clumping' is determined by measuring the $^{13}C^{18}O^{16}O$, $^{12}C^{18}O^{17}O$, and $^{13}C^{17}O^{17}O$ isotopologues of CO_2 (collectively comprising the mass 47 ion beam, with the vast majority of species at that mass being $^{13}C^{18}O^{16}O$) extracted from a carbonate mineral via reaction with concentrated phosphoric acid. It is reported as a Δ_{47} value, which is the enrichment of the mass 47 isotopologue in a sample relative to a stochastic distribution of isotopes (Eiler and Schauble, 2004; Wang et al., 2004).

Most of the published measurements of clumped isotopes have been obtained from calcite- or aragonite-bearing materials, and there is no consensus yet on whether the existing calcite calibrations are appropriate for other minerals. Guo et al. (2009) used the theoretical predictions of Schauble et al. (2006) and a model of kinetic effects during phosphoric acid digestion of carbonates to calculate the temperature vs. Δ_{47} relationship for several carbonate minerals. They predict that several types of carbonates are offset from the calcite calibration to lower or higher Δ_{47} values. Their work does not include a prediction for siderite because Schauble et al. (2006) did not consider this mineral in their calculations; however, they do provide an estimate for the Δ_{47} value expected in CO_2 extracted at 25 °C from siderites with a stochastic distribution of ^{13}C–^{18}O bonds. Their estimate shows that the siderite calibration should be offset to lower Δ_{47} values by approximately 0.03‰ relative to calcite (outside the accepted external reproducibility of clumped isotope measurements of 0.02‰). This prediction, however, has not been validated by empirical studies of siderites grown in the laboratory at known temperatures.

Additionally, there are no empirical studies that show what effect the temperature of phosphoric acid digestion has on Δ_{47} values for minerals other than calcite. Siderites are commonly reacted at elevated temperatures because acid digestion of siderite can be extremely slow at 25 °C (on the order of days or weeks, e.g., Rosenbaum and Sheppard, 1986). The most widely used calibration (Ghosh et al., 2006) was generated from calcite samples reacted at 25 °C, and siderite data generated at elevated acid digestion temperatures (>25 °C) must first be normalized to that reaction temperature in order to use any of the existing (both empirical and theoretical) carbonate calibrations.

Here we present an inorganic calibration for the siderite clumped isotope paleothermometer using minerals precipitated in the laboratory under controlled temperature conditions. We demonstrate that this calibration is indistinguishable from calcite at current levels of analytical precision. We also present clumped isotope measurements of a natural siderite sample collected from Holocene sediments of the Mississippi River Delta that suggest that siderites record warm season marsh water temperatures instead of MAATs as has long been presumed.

2. METHODS

2.1. Synthetic siderite

Siderite was precipitated under controlled temperature conditions (4, 9, 21, 39, 51 ± 1 °C) following the procedures of Wiesli et al. (2004) who used a method similar to that described by Kim and O'Neil (1997) for Ca, Cd, and Ba carbonates, along with several precautions intended to prevent oxidation of dissolved Fe(II). The reactor temperature was controlled with the aid of a temperature controlled water bath (Fisher Scientific®, Isotemp 110), which has an observed precision of ±1 °C. Experimental solutions of $FeCl_2$ and $NaHCO_3$ were prepared in two Erlenmeyer flasks using 18 MΩ water that had been made anoxic by continuous flushing with N_2 for ~2 h (Fig. 1). The N_2 was first bubbled through water to saturate the gas and minimize evaporation in the experimental solutions. One flask contained 100 ml of a 0.05 mM solution of $FeCl_2$ and the other 300 ml of a 0.05 mM solution of $NaHCO_3$. Both flasks were acidified until the $NaHCO_3$ solution reached a pH ~ 6.7 by

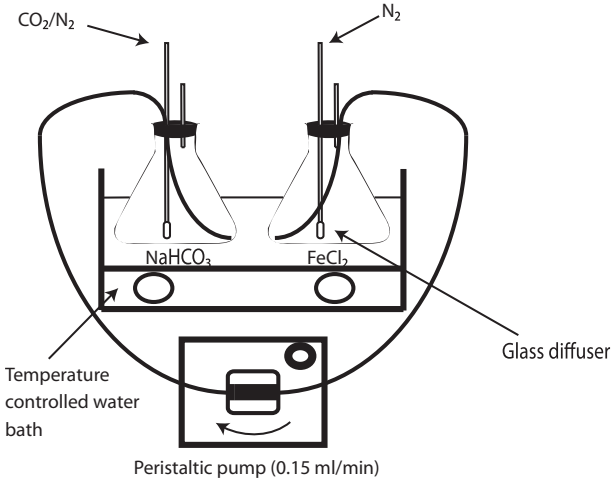

Fig. 1. Schematic of the experimental apparatus used for siderite synthesis experiments. An $FeCl_2$ solution was slowly titrated into a flask containing a $NaHCO_3$ solution. Precipitation was achieved by degassing of CO_2. See text for details.

vigorously flushing with CO_2 for 4–5 h. This step also allowed the solutions to equilibrate to the experimental temperature. At this point the $FeCl_2$ solution was slowly titrated (0.15 ml/min) into the $NaHCO_3$ solution using a peristaltic pump.

Once all of the Fe solution was transferred into the other flask, precipitation was allowed to begin by gently flushing the solution with N_2 gas and increasing pH. Experiments were allowed to proceed for 24–90 h after the end of the titration step. At this point enough precipitate (~300–350 mg) had formed for XRD and clumped isotope analysis. At the end of the experiments precipitates were filtered through a syringe filter fitted with a 0.2 μm quartz fiber filter under a N_2 atmosphere inside of a glove bag. The filters were rinsed with anoxic DI water and placed inside of a Vacutainer®. The containers were dried by attaching them to a vacuum line with the aid of a hypodermic needle. An aliquot of the precipitates (150 mg) and experimental waters was saved for X-ray diffraction and $\delta^{18}O$ analyses, respectively.

2.2. Natural siderites

Siderite samples were collected from Holocene sediments of the Mississippi River Delta (Fig. 2) from cores drilled using a hand operated Edelman auger with a 3 cm gouge. Sediment texture was described in the field following US Department of Agriculture (USDA) classification. Siderite is present in these sediments as centimeter-sized concretions composed of finely disseminated carbonate crystals within a fine mud matrix. Carbonate nodules were separated by hand and allowed to dry overnight in a 60 °C oven. The samples were then crushed with a synthetic sapphire mortar and pestle (Diamonite™) and sieved through a 108 μm mesh. An aliquot of this powder (500 mg) was submitted for X-ray diffraction analysis.

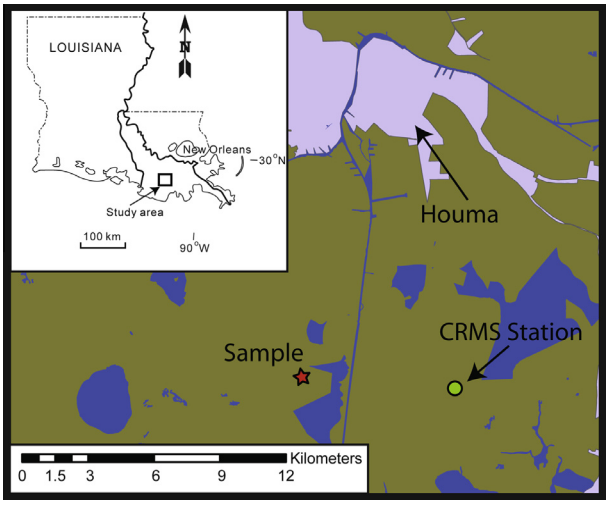

Fig. 2. Map showing coring locations for natural siderite samples (latitude: 29.476, longitude: −90.738) in the Mississippi River Delta, USA (sample). The locations of the stations that provided the water temperature record (CRMS station #392) and the air temperature record (Houma-Terrebonne Station, NOAA) are also shown.

2.3. CO_2 sample preparation for mass spectrometric analysis

15–40 mg of powdered carbonate samples were reacted with concentrated phosphoric acid (1.95 g/ml) at 100 °C in a two-legged, McCrea-type reaction vessel submerged in boiling water. The sample and acid were allowed to equilibrate for approximately 20 min before tipping the acid reservoir to react with the powdered mineral. Sample CO_2 was continually trapped in a 4-loop trap held under liquid nitrogen while the reaction was allowed to proceed. Reaction times ranged between 15 and 45 min depending on the grain size of the powdered sample and mineralogy (siderite samples vs. calcite standards). At the end of the reaction, water was separated from the sample gas by warming the trap with an isopropyl alcohol slush (−70 °C). The gas was then passed twice through a trap filled with PoraPak® resin and silver wool held at −15 °C with ethylene glycol at the solid–liquid phase transition (see Rosenheim et al., 2013 for more detail on sample preparation) to remove hydrocarbon/halocarbon impurities that can create isobaric interferences during mass spectrometry (Eiler and Schauble, 2004).

2.4. Mass spectrometry

Clumped isotope measurements were performed at Tulane University using a 5Kv Isoprime® dual inlet isotope ratio mass spectrometer (IRMS) following the procedures described in Rosenheim et al. (2013). This system is fitted with 6 Faraday cups configured for simultaneous detection of masses 44–49 m/z. Samples of CO_2 were introduced to the IRMS by freezing them into a small volume using liquid nitrogen. The pressure in the bellows was adjusted to yield 100 nA in the mass 44 m/z cup. Samples were measured for 24 acquisitions of 5 reference gas-sample gas comparisons with a 12 s delay and a 20 s integration time, in some cases following determination of the pressure baseline (He et al., 2012) for each acquisition. Total integration time for each sample gas is 1200 s.

All Δ_{47} data presented in this paper is reported in the absolute scale of Dennis et al. (2011) using CO_2 heated (1000 °C) and equilibrated with water at various temperatures (50, 28, and 4.5 °C – see Rosenheim et al., 2013 for more details on particular reference frames in our laboratory). Clumped isotope data were obtained during two analytical sessions, May–August 2012 and January–March 2013. Machine drift and changes in scale stretching/compression effects were monitored by measuring equilibrated gases and carbonate standards along with the unknowns.

The data from the 2012 analytical session (a subset of sessions presented in Rosenheim et al., 2013) exhibited a slight linearity between Δ_{47} and bulk isotopic composition (~0.01 Δ_{47} per δ^{47}); these data were corrected using typical correction algorithms as described by Huntington et al. (2009) and Dennis et al. (2011). The data from the 2013 analytical session were obtained after the source filament was replaced. These data exhibited increased linearity

between Δ_{47} and bulk isotopic composition (~0.05 Δ_{47} per δ^{47}). The effect was judged as too large to be reliably corrected using traditional algorithms because small variations in the Δ_{47} vs. δ^{47} relationship are not easily detected when the slope is large. In this case, data were first corrected by subtracting measurements of the pressure baseline (PBL, He et al., 2012) that is registered as negative background in the Faraday detectors when CO_2 is measured off-peak (~41 V off peak in the case of our IRMS; see He et al., 2012; Bernasconi et al., 2013; Rosenheim et al., 2013). This effectively reduced the slope of the Δ_{47} vs. δ^{47} relationship to −0.002 and eliminated the uncertainties associated with machine drift (see Rosenheim et al., 2013 for how this affects precision of carbonate standards). The correction routine was modeled after He et al. (2012) except that the PBL was measured for both the sample and the reference gas only once before every acquisition because we observe that the PBL does not change appreciably with the gas depletion that occurs during one acquisition block. After subtraction of the PBL, the data were projected into the absolute scale following Dennis et al. (2011).

Stable carbon and oxygen isotope abundances were determined using the raw current measurements from cups 44–46 and the algorithm of Santrock et al. (1985). Siderite $\delta^{18}O$ data were corrected for acid digestion at 100 °C using the acid fractionation factors of Rosenbaum and Sheppard (1986), and calcite $\delta^{18}O$ data using the fractionation factors reported by Swart et al. (1991). A clumped isotope acid fractionation of 0.106‰ was used for our calcite standards to account for our acid digestion temperature of 100 °C. This value is a linear extrapolation of the acid fractionation at 90 °C (0.092 ± 0.012) reported by Henkes et al. (2013).

External reproducibility for both stable and clumped isotope measurements was explored by replicate measurements of unknown samples and by repeated measurements of carbonate standards. Two carbonate reference materials available from the IAEA (IAEA-CO1 and IAEA-C1) and one internal laboratory standard (CORS, Rosenheim et al., 2013) were measured for this purpose. IAEA-CO1 and IAEA-C1 are both Carrara marble standards distributed by the IAEA; both were prepared from the same slab of Carrara Marble and are distributed as a stable isotope and radiocarbon standard, respectively. These standards have a combined Δ_{47} value of 0.391 ± 0.006‰ ($n = 19$, 1 s.e, 0.027 s.d.), which is consistent with values obtained for Carrara marbles by other laboratories (Dennis et al., 2011). The CORS standard was prepared from coral rubble from Hawaii that was homogenized and sieved to yield a 108 μm fraction. We measure this standard to test reproducibility across analytical sessions, and it has an average value of 0.737 ± 0.005‰ ($n = 21$, 1 s.e., 0.022 s.d.). The precision of these standards is slightly lower than the average precision obtained for siderite measurements of 0.01‰ (1 s.e.).

Measurements of water $\delta^{18}O$ were performed on the same instrument using an automated Multiprep equilibration device. For each sample 200 μL of water were equilibrated with CO_2 (for 5 h) in an ~8 ml glass vial with a septum cap. Equilibrated gases were automatically expanded into a water trap held at −70 °C before being admitted to the sample bellows and the ion source. IAEA standards SMOW, SLAP and GISP were included in each run along with calibrated internal laboratory standards. Raw data was normalized and corrected for drift and memory effects.

3. RESULTS

3.1. Siderite precipitation experiments

Siderite was the only phase detected in the XRD spectra of experiments conducted at 21, 39 and 51 °C (Fig. 3); although, we cannot rule out the possibility that other phases were present below the XRD detection limit of approximately 3%. Minerals precipitated at lower temperatures (4 and 9 °C) did not conform to siderite XRD spectra although they did effervesce with acid. No additional analyses were done on these two low temperature experiments. The failure of these experiments to produce siderite is not surprising considering the apparent slow growth kinetics of siderite at low temperatures and the lack of reports in the literature of successful siderite precipitation experiments at temperatures less than 17 °C (e.g., Jimenez-Lopez and Romanek, 2004).

The powders from the successful experiments were observed to be weakly magnetic likely due to the presence of small amounts of magnetite not detected by XRD analyses (Fig. 3). Magnetite has also been reported in other siderite synthesis experiments (Zhang et al., 2001), and in this case it is likely the result of trace amounts of oxygen in the experimental fluids. The presence of magnetite does not

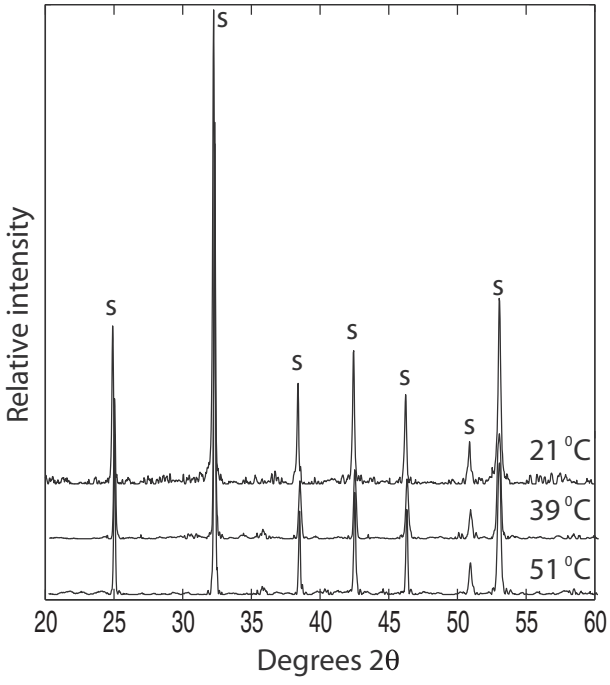

Fig. 3. X-ray diffraction patterns showing prominent siderite peaks (*s*) for the experiments conducted at 21, 39 and 51 °C. No crystalline phases were detected in the two low temperature experiments (4 and 9 °C).

affect the values obtained for clumped isotopes because it does not release CO_2 during phosphoric acid digestion.

3.2. Stable and clumped isotopes

Stable isotope, $\delta^{18}O$ values for the experimental waters, and clumped isotope values are presented in Table 1. The siderite-water oxygen isotope fractionations for our experiments are consistent with the relationship reported for abiotic siderite by Carothers et al. (1988). The 21 °C experiment shows an isotope fractionation larger than expected; however, the difference from the existing calibration is not statistically significant (Fig. 4). It is possible that this sample does capture the actual siderite equilibrium fractionation, and the mismatch occurs because the Carothers et al. (1988) relationship is extrapolated to low temperatures. While it is generally not possible to prove that stable isotope equilibrium was reached in a laboratory experiment (Kim and O'Neil, 1997), we show agreement between our results and previously published data that are thought to be representative of equilibrium conditions.

Least square linear regression of siderite Δ_{47} values and temperature ($10^6/T^2$, K) yields the following relationship ($r^2 = 0.997$):

$$\Delta_{47\text{-RF}} = \frac{(0.0356 \pm 0.0018) \times 10^6}{T^2} + (0.172 \pm 0.019) \quad (1)$$

The slope of this equation is statistically indistinguishable to the slope reported by Dennis and Schrag (2010) for calcite precipitation experiments ($m = 0.0362 \pm 0.0018$) and to the slope predicted by Schauble et al. (2006) for the temperature dependence of clumping in the calcite mineral lattice between 0 and 70 °C ($m = 0.0392$). The slope of this relationship is, however, different than the equation of Ghosh et al. (2006), which accurately describes the temperature sensitivity of many types of natural samples ($m = 0.0636 \pm 0.0049$) (e.g., Eiler, 2011, Fig. 2 and references therein).

The intercept of our calibration depends on the temperature of phosphoric acid reaction, with lower acid-digestion temperatures resulting in higher Δ_{47} values and larger intercepts. In this case, our siderite data are offset from the existing calcite calibrations because the existing calcite equations are reported at reaction temperatures of 25 °C. To compare these to our data, the calcite calibrations can be normalized to 100 °C by subtracting an appropriate acid correction factor. This approach, however, confounds any mineral specific differences that may exist with uncertainties related with the correction factor.

A better approach is to directly compare our data with calcites grown at known temperatures and reacted at 100 °C. This is done graphically in Fig. 5, which plots our siderite data along with the results for inorganic calcite precipitation experiments reported by Tang et al. (2013). These calcite samples offer the added benefit of having been analyzed at the same time and using the same methods as our siderite samples, so they can also be used to rule out any inter-laboratory bias. In this case, both the slope (0.0387 ± 0.0072) and the intercept (0.147 ± 0.083) of the calcite calibration of Tang et al. (2013) are statistically indistinguishable to the slope and intercept of our siderite calibration. Moreover, both calibrations are within statistical error of the slope of the theoretical calcite calibration ($m = 0.0392$).

3.3. Natural siderite

One natural siderite sample was measured with a Δ_{47} value of 0.556 ± 0.003 (Table 2), this corresponds to a temperature of 31.3 ± 1.3 (1 s.e.) using Eq. (1). This temperature is significantly higher than the present average air temperature of 20.8 °C, measured in a weather station located approximately 20 km from the sampling site (Houma-Terrebonne Station, NOAA, National Climatic Data Center). The clumped temperature estimate is indistinguishable from to the mean warm season (June–August) marsh water temperature 29.2 ± 1.3 (1σ) measured in station #392 of the Coastwide Reference Monitoring System-Wetlands (CRMS-Wetlands) of the Louisiana Office of Coastal Protection and Restoration (Fig. 6). This station is located approximately 7 km from the sampling site.

4. DISCUSSION

4.1. Differences between calcite and siderite

No existing theoretical calculation quantitatively predicts how the siderite Δ_{47} vs. temperature equilibrium relationship would compare to that of calcite, but we can use existing theoretical relationships for other carbonate minerals to estimate the general direction that this calibration should assume. The abundance of ^{13}C–^{18}O bonds in CO_2 derived from phosphoric acid digestion of carbonate minerals is proportional to their abundance in the mineral lattice plus a temperature dependent acid fractionation factor:

$$\Delta_{47\text{-eq}}^{CO_2\text{-}XCO_3} = \Delta_{63\text{-eq}}^{XCO_3} + \Delta_{47\text{-}XCO_3}^{*} \quad (2)$$

In this case a prediction for siderite $\Delta_{63\text{-eq}}$ can be made based on the work of Schauble et al. (2006) who used first-principle lattice dynamics to calculate the temperature dependence of clumping in different carbonate minerals. Their calculations do not include predictions for siderite, but they predict that equilibrium constants for the different minerals they studied are only slightly different at any given temperature. For instance, they show a total range of approximately 0.024‰ in Δ_{63} values at 25 °C (dolomite–aragonite). However, the small variations that they do observe are not random and instead depend on the crystal structure of the mineral (e.g., calcite vs. aragonite) and on the atomic number of the cation in the carbonate mineral (e.g., magnesium vs. calcium). Based on the larger atomic number of iron relative to calcium we expect the siderite Δ_{63} vs. temperature relationship to be offset by a small amount to lower values relative to calcite (i.e. $\Delta_{63\text{-eq}}^{CaCO_3} - \Delta_{63\text{-eq}}^{FeCO_3} > 0$).

We do not yet know to what extent the acid digestion fractionation factor (Δ_{47}^{*}) in Eq. (2) varies for the different carbonate minerals, but we do know that its value depends on the temperature of acid digestion (Ghosh et al., 2006). This factor can be estimated by experiments (e.g., Ghosh et al., 2006; Guo et al., 2009; Passey and Henkes, 2012) or by theoretical calculations. Guo et al. (2009) report

Table 1
Stable isotopes and clumped isotope results for siderite synthesis experiments.

Run#	Temperature[a]	Duration	$\delta^{13}C_{PDB‰}$ siderite	$\delta^{18}O_{SMOW‰}$ siderite	$\Delta_{47‰}$[b]	SE[c]	$\delta^{18}O_{SMOW‰}$ water[d] ($\pm1\sigma$)	Temperature[e] ($\pm1\sigma$)
190	21 ± 1 °C	65 h	7.61	27.48	0.603	0.009	−6.4 ± 0.4	16.2 ± 2.4
357			7.62	28.13	0.582	0.013		
378			7.63	27.91	0.568	0.010		
Average			7.62	27.84	0.584			
Standard error			0.01	0.19	0.010			
186	39 ± 1 °C	46 h	3.97	22.61	0.546	0.009	−5.9 ± 0.2	41.1 ± 1.5
373			4.01	22.45	0.501	0.011		
383			4.03	22.46	0.543	0.013		
386			4.03	22.45	0.548	0.013		
Average			4.01	22.49	0.535			
Standard error			0.01	0.04	0.011			
187	51 ± 1 °C	36 h	2.22	19.72	0.491	0.009	−6.1 ± 0.4	54.5 ± 3.3
362			2.14	19.65	0.463	0.011		
379			2.22	19.80	0.553	0.012		
382			2.21	19.72	0.498	0.014		
387			2.22	19.70	0.553	0.012		
Average			2.20	19.72	0.512			
Standard error			0.02	0.02	0.018			

[a] Temperature during the precipitation experiments. Uncertainty is the observed stability of the temperature controlled water bath.
[b] Clumped isotope measurements in the absolute reference frame (Dennis et al., 2011) at 100 °C acid digestion temperature.
[c] Reported uncertainty is the internal standard error from counting statistics of a single measurement.
[d] Measured $\delta^{18}O$ of water used in experiments. Reported uncertainty is the standard deviation of replicate samples.
[e] Temperature estimated using the siderite-water oxygen isotope equilibrium equation of Carothers et al. (1988). Error in temperature estimate reflects the propagated analytical uncertainty of the oxygen isotope composition of the siderite samples and of the experimental solutions.

estimates for Δ^*_{47} fractionations for different carbonate minerals based on a model for kinetic isotope effects during phosphoric acid digestion that they calculate using transition state theory and statistical thermodynamics. Their model predicts a smaller value for the siderite fractionation factor than their value for calcite. In other words, if a particular siderite and calcite sample have the same amount of clumping in their lattice, more ^{13}C–^{18}O bonds are present in the CO_2 derived from the calcite sample than that from the siderite sample ($\Delta^*_{47\text{-}CaCO_3} - \Delta^*_{47\text{-}FeCO_3} = 0.027$; Table 4 in Guo et al., 2009).

Subtracting an expression for calcite using Eq. (2) with a similar expression for siderite and rearranging yields:

$$\Delta_{47\text{-eq}}^{CO_2-CaCO_3} - \Delta_{47\text{-eq}}^{CO_2-FeCO_3} = \left(\Delta_{63\text{-eq}}^{CaCO_3} - \Delta_{63\text{-eq}}^{FeCO_3}\right) + \left(\Delta^*_{47\text{-}CaCO_3} - \Delta^*_{47\text{-}FeCO_3}\right) \quad (3)$$

$$\Delta_{47\text{-eq}}^{CO_2-CaCO_3} - \Delta_{47\text{-eq}}^{CO_2-FeCO_3} > 0.027‰ \quad (3.1)$$

Eq. (3.1) shows that at a given temperature siderites should have lower Δ_{47} values relative to calcite by a minimum of 0.027‰. We do not observe an offset from calcite in our experimental results. The root mean square error (RMSE) of the residuals (a measure of goodness of fit) calculated between the values predicted by the inorganic calibration of Tang et al. (2013) and the Δ_{47} values of our siderite samples is 0.008‰. The RMSE is roughly equal to our external precision in clumped isotope measurements as judged by our secondary calcite standards (0.006‰, see Section 2 and Rosenheim et al., 2013 for more details) and our average precision for siderite measurements of 0.01‰. In other words, the small differences that we observe between siderite and calcite samples can be explained by analytical uncertainties. This observation implies that the result of Eq. (3.1) is smaller than our analytical error, and the difference in magnitudes predicted by Guo et al. (2009) for the acid-digestion fractionations for calcite and siderite is probably not accurate.

Our results support previous observations that there is no resolvable difference between the clumped isotope calibrations of some carbonate minerals. Eagle et al. (2010) present a thermodynamic model of clumped isotope equilibrium in apatite along with Δ_{47} measurements of apatite samples grown at known temperatures. Their experimental calibration is statistically indistinguishable from the calcite calibration of Ghosh et al. (2006), and their thermodynamic calculations for equilibrium clumping in the apatite mineral lattice agree with their calculations for calcite within approximately 0.004‰ (or ~1.5 °C). Similarly, measurements of aragonite materials grown at known temperatures

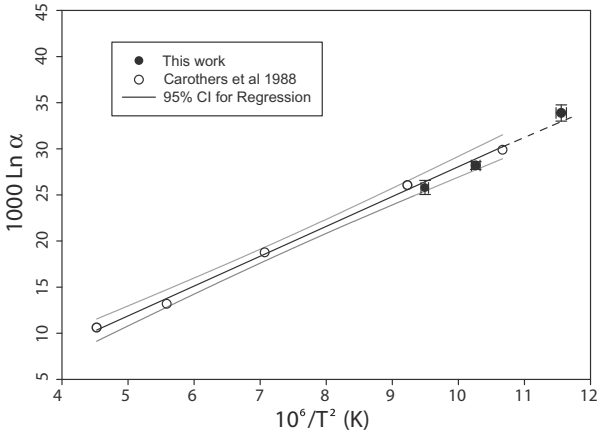

Fig. 4. Oxygen isotope ($\delta^{18}O$) fractionation between siderite and water. Plot includes the 95% confidence interval for the slope and the intercept of the equilibrium equation of Carothers et al. (1988).

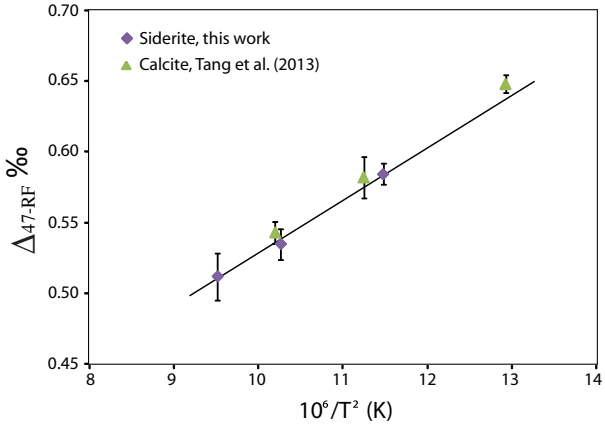

Fig. 5. Linear regression of the siderite clumped isotope results and temperature (Eq. (1)). The figure also includes the results for synthetic calcite samples of (Tang et al., 2013). These calcite samples were measured during the same time period as the siderite samples and are shown at an acid digestion temperature of 100 °C.

show no offsets from the calcite calibrations that can be unambiguously attributed to mineralogical differences (Tripati et al., 2010; Thiagarajan et al., 2011; Eagle et al., 2013). All of these observations combined suggest that carbonates faithfully record the clumped isotope signature of the dissolved inorganic carbon from which they form instead of mineral specific clumped isotope equilibrium, and importantly that there is no large systematic difference in acid-digestion fractionations for different carbonate minerals. As precision of Δ_{47} determinations increases, this will undoubtedly be re-evaluated, but at current analytical precisions differences between minerals are simply too small to be detected.

4.2. Inconsistent slopes for clumped isotope calibrations

One of the most important and still unresolved issues facing the clumped isotope community is the reason behind inconsistent slopes in empirical calibrations (Ghosh et al., 2006; Dennis and Schrag, 2010). The majority of the published calibration data was measured in a single laboratory (Caltech) and generally conforms to a calibration with a steep slope, 'Ghosh' calibration. However, the first results published by another laboratory (Dennis and Schrag, 2010) are more consistent with a calibration of shallower slope, 'Dennis and Schrag' calibration. Most workers assume that equilibrium is better described by the 'Ghosh' calibration mainly due to the quantity and diversity of data that conforms to this relationship (e.g., Eiler, 2011). A growing number of datasets coming from other laboratories (Dennis and Schrag, 2010; Eagle et al., 2013; Henkes et al., 2013; Tang et al., 2013; and this work) are beginning to challenge this assertion. Although a definitive explanation for these disagreements is outside of the scope of this work, a discussion that places our results in the context of this ongoing debate is warranted.

One possible hypothesis is that only one relationship represents true clumped isotope equilibrium; whereas, the other one records kinetic isotope effects in the dissolved inorganic carbon (DIC) pool. Kinetic effects are most likely to occur at lower temperatures because of the slower isotope exchange kinetics between DIC and water, and it is at low temperatures where the two calibrations are dissimilar. For instance, Beck et al. (2005) reported that at the pH levels where DIC is dominated by HCO_3^- (a similar condition as our siderite experiments, and the experiments of Ghosh et al. (2006), Dennis and Schrag (2010) and Tang et al. (2013)) isotopic equilibrium with water takes about 2 h at 40 °C vs. 24 h at 15 °C. Thus, kinetic effects are most likely to be recorded in the experiments with the fastest precipitation rates where CO_3^{2-} precipitates before reaching isotope equilibrium with water.

Table 2
Stable isotope and clumped isotope results for a natural siderite from the Mississippi River Delta.

Run#	$\delta^{13}C_{PDB‰}$	$\delta^{18}O_{SMOW‰}$	$\Delta_{47‰}$ [a]	SE[b]	Temperature ($\Delta_{47‰}$)[c]
401	−7.61	29.25	0.556	0.011	31.4
404	−7.59	29.31	0.551	0.011	33.4
428	−7.57	29.24	0.562	0.013	29.1
Average	−7.59	29.27	0.556		31.3
Standard error	0.01	0.02	0.003		1.3

[a] Clumped isotope measurements in the absolute reference frame (Dennis et al., 2011).
[b] Reported uncertainty is the internal standard error from counting statistics of a single measurement.
[c] Temperature estimated using Eq. (1) for siderites digested at 100 °C.

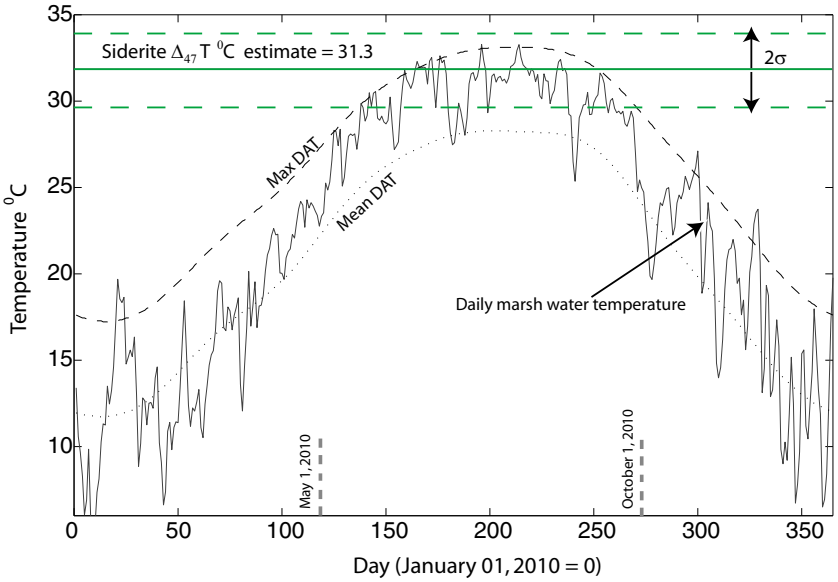

Fig. 6. Clumped isotope temperature estimate for a natural siderite sample from the Mississippi River Delta, USA. The 2σ is the standard error of Δ_{47} values for three separate CO_2 extractions. Also plotted is the daily marsh water temperature close to the sampling site (CRMS station #392) for the year 2010, the long term mean of daily average air temperature (mean DAT) and the long term mean of daily maximum air temperature (Max DAT) for the year 2010 (Houma-Terrebonne Station, NOAA; see Fig. 2).

Ghosh et al. (2006) and Dennis and Schrag (2010) do not report precipitation rates for their experiments, but it is reasonable to assume that faster precipitation rates occur in the active degassing experiments of 'Ghosh' vs. the passive degassing experiments of 'Dennis and Schrag'. Similarly, faster precipitation rates are expected in our siderite experiments vs. the slower CO_2 diffusion method of Tang et al. (2013). The problem with this hypothesis is that both 'Ghosh' and 'Dennis and Schrag' report $\delta^{18}O$ values for their low temperature samples that seem to be close to equilibrium with experimental fluids but have widely dissimilar Δ_{47} values. Likewise, we report siderite $\delta^{18}O$ values that suggest oxygen isotope equilibrium. More importantly, Tang et al. (2013) see precipitation-rate related offsets from oxygen isotope equilibrium in the range of precipitation rates they studied ($\log R = 1.8$–4.4 $\mu mol/m^2/h$) but report Δ_{47} values that are well within analytical uncertainty of each other.

We believe these observations suggest that clumped isotopes are not sensitive to small deviations from oxygen isotope equilibrium between DIC and water, at least at the precision that we can currently measure Δ_{47} values. It follows that both the 'Dennis and Schrag' and 'Ghosh' calibrations represent clumped isotope equilibrium. This interpretation is also supported by Δ_{47} measurements of deep sea corals, which are notorious for non-equilibrium isotope effects (Weber, 1973; Smith et al., 2000; Adkins et al., 2003, among others) but nevertheless show apparent clumped isotope equilibrium (Ghosh et al., 2006; Thiagarajan et al., 2011).

It seems counterintuitive to suggest that both calibrations represent clumped isotope equilibrium, but one possibility is that the differences that we observe are related to the methods used to prepare samples for mass spectrometric measurement of clumped isotopes. The strongest evidence for this interpretation is the observation that calibration data plot into two distinct populations depending on the method used for acid digestion. The published calibration data that conform to the 'Ghosh' calibration were measured in Caltech using a temperature of 25 °C for phosphoric acid-digestion. In this case, carbonate samples were reacted in McCrea-type reaction vessels and the reaction was allowed to proceed overnight before removal of CO_2, GC sample purification, and mass spectrometric analysis (e.g., Ghosh et al., 2006; Huntington et al., 2009). On the other hand, the carbonates that conform to the 'Dennis and Schrag' calibration were reacted at 70–100 °C and the resulting CO_2 was actively removed as the reaction proceeds.

This point is illustrated in Fig. 7a where we plot Δ_{47} values for carbonates digested at high temperatures. Note that this figure includes the bioapatite data of Eagle et al. (2010), originally interpreted to conform to the 'Ghosh' calibration, and the cephalopod data of Dennis et al. (2013) that were interpreted as falling outside clumped isotope equilibrium. A linear regression was performed on the combined data set and resulted in the following relationship ($r^2 = 0.67$):

$$\Delta_{47\text{-RF}} = \frac{(0.0385 \pm 0.0019) \times 10^6}{T^2} + (0.271 \pm 0.023) \qquad (4)$$

Fig. 7a includes the 95% confidence interval for new observations, which was calculated assuming a standard deviation equal to the external inter-laboratory reproducibility of clumped isotope measurements of 0.02‰ (Dennis et al., 2011). Most of the data plots within this interval suggesting that the spread around the regression line is related to analytical uncertainties alone.

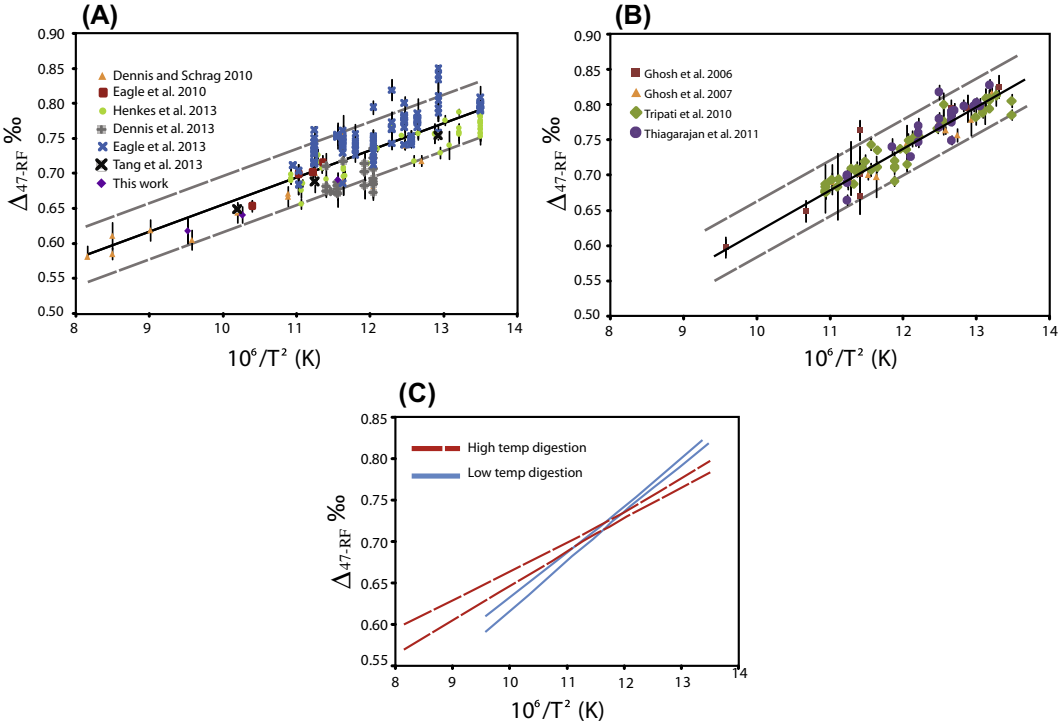

Fig. 7. (A) Linear regression of carbonate samples digested at high temperatures and active removal of CO_2. (B) Linear regression of carbonate samples digested at low temperature. The 95% confidence interval for new observations, calculated assuming an external reproducibility of 0.02‰, is included in both (A) and (B). (C) 95% confidence intervals for regression coefficients of Eqs. (4) and (5). Note: all data are presented in the absolute reference frame at an acid digestion temperature of 25 °C. Data that were not originally published in the absolute reference frame were obtained from Eagle et al. (2013) (see their supplementary materials for details of how data was scaled to the absolute reference frame and corrected for acid digestion temperature). Our siderite data and the calcite data of Tang et al. (2013) were normalized to 25 °C by adding 0.106‰ (see Section 2) (See Panel B for Ghosh et al., 2007).

On the other hand, carbonates digested at low temperature follow a steeper slope similar to the slope of the 'Ghosh' calibration ($r^2 = 0.91$):

$$\Delta_{47\text{-RF}} = \frac{(0.0574 \pm 0.0019) \times 10^6}{T^2} + (0.051 \pm 0.024) \qquad (5)$$

These data are plotted in Fig. 7b along with the 95% confidence interval for new observations calculated as in Fig. 7a. The data plot within this interval suggesting, again, that the spread is related to analytical uncertainties. Moreover, the difference between the slopes of the two groups (Eqs. (4) and (5)) is significantly different in an analysis of covariance (ANCOVA) test ($p < 0.0001$) (Fig. 7c).

It is not clear what aspect of the acid digestion reaction affects the clumped isotope composition of the CO_2 that is released, or why it only seems to affect samples with a more enriched clumped isotope composition (i.e. low temperature samples). One possibility is that the clumped isotope acid fractionation factor (Δ^*_{47}) varies with the method of acid digestion much like oxygen isotope fractionations. For instance, Swart et al. (1991) determined the temperature dependence of oxygen isotope fractionations for two commonly used methods of acid digestion (closed vessel vs. active removal of CO_2). They found that the two methods produce values that are offset from each other by as much as 0.4‰. Eagle et al. (2013) recently suggested that discrepancies between calibrations may be the result of fractionations during sample purification that preferentially affect samples with an enriched clumped isotope composition. Both possibilities should be investigated by a systematic inter-laboratory comparison of carbonate samples over a wide range of bulk isotope and Δ_{47} compositions prepared in different ways. In any case, we observe that the siderite Δ_{47}-temperature calibration is indistinguishable from both theoretical and empirical calcite calibrations (Schauble et al., 2006; Passey and Henkes, 2012; Tang et al., 2013).

4.3. Natural siderites

Siderites from the Mississippi River Delta record clumped isotope temperatures in excess of MAATs. Clumped isotope temperatures correspond more closely to marsh water temperatures during the summer months (Fig. 6). This seasonal bias is similar to that observed for pedogenic calcite (Passey et al., 2010; Peters et al., 2013); although, in those cases it occurs because calcites form during warm and dry periods when soil water loss and degassing of CO_2 increase the saturation state of calcite (Breecker et al., 2009).

The bias for siderites precipitating during the warmest parts of the year in southern Louisiana marshes may be explained by higher rates of microbial respiration and organic

matter decomposition when soil temperatures are hotter. Siderites form after dissimilatory iron reducing bacteria mobilize ferrous iron and release CO_2 from the oxidation of organic matter (Mortimer and Coleman, 1997; Ludvigson et al., 1998). During the summer, increased bacterial activity leads to larger concentrations of dissolved Fe(II) and CO_3^{2-} and to a reduction in siderite solubility. Siderite with a clumped isotope composition reflecting summer high temperatures would be expected to precipitate during these periods of reduced solubility.

The observation that siderites form during the summer and do not record MAATs has important implications for the accuracy of stable isotope- and clumped isotope-based climate reconstructions, and it may explain reports in the literature of deviations from the siderite-water oxygen isotope equilibrium relationship of Carothers et al. (1988) in some natural samples. For instance, Driese et al. (2010) use siderite $\delta^{18}O$ values along with the MAAT (15.8 °C) for a site in Chattanooga, Tennessee, USA, and calculate soil water $\delta^{18}O$ values. They show a mismatch between their calculated oxygen isotope composition for soil waters and the values expected from the oxygen isotope composition of local precipitation. The discrepancy that they report, however, can be resolved if a temperature closer to the mean summer (May–September) air temperature of 21.6 °C (Chattanooga Lovell Field Airport, TN, NOAA-National Climatic Data Center) is used instead of the MAAT (see their Fig. 8).

More recently, Ludvigson et al. (2013) reported soil water temperatures and $\delta^{18}O_w$ compositions for the Driese et al. (2010) site during March and August of 2010. The March temperatures and $\delta^{18}O_w$ values they present clearly fall outside of the range predicted by the isotopic compositions of siderites at the site and the Carothers et al. (1988) equation. To explain this they argue that the equation of Zhang et al. (2001) may be more representative of oxygen isotope equilibrium at low sedimentary temperatures (<30 °C). While this is certainly possible, we note that the disagreement between their field data and the Carothers et al. (1988) equation is not as severe if a warm season bias for siderite formation is taken into account.

5. CONCLUSIONS

Data presented in this paper show that there is no resolvable difference in the Δ_{47} vs. temperature relationship between calcite and siderite. Our observations suggest that there is likely no large systematic bias in the clumped isotope acid fractionation factors between two different carbonate minerals, siderite and calcite. These results imply that we may be able to obtain accurate temperature estimates using clumped isotope thermometry from samples of complex mineralogy (i.e. mixed mineralogy samples and solid solutions), especially in cases where various minerals precipitate in the same water and at the same temperature.

We measured the clumped isotope composition of a natural siderite collected from the Mississippi River Delta. Temperature estimates for this sample are significantly higher than local mean annual air temperatures. Our estimate shows a seasonal bias close to the temperature of the soil waters during the summer. This suggests that siderites form during periods of increased microbial soil respiration, which occur during the summer months when soil temperatures are higher. This observation has important implications for the use isotopic signals from siderites in climate reconstructions.

ACKNOWLEDGMENTS

These analyses were funded by the Department of Earth and Environmental Sciences (materials and supplies) and by the School of Science and Engineering (technician support for J. Tang) at Tulane University. A. Fernandez was supported with funds from the Oliver Fund and the Vokes Fellowship at Tulane University. We thank two reviewers and the Associate Editor for improving this manuscript.

REFERENCES

Adkins J. F., Boyle E. A., Curry W. B. and Lutringer A. (2003) Stable isotopes in deep-sea corals and a new mechanism for "vital effects". *Geochim. Cosmochim. Acta* **67**, 1129–1143.

Beck W. C., Grossman E. L. and Morse J. W. (2005) Experimental studies of oxygen isotope fractionation in the carbonic acid system at 15°, 25°, and 40 °C. *Geochim. Cosmochim. Ac.* **69**, 3493–3503.

Bernasconi S. M., Hu B., Wacker U., Fiebig J., Breitenbach S. F. M. and Rutz T. (2013) Background effects on Faraday collectors in gas-source mass spectrometry and implications for clumped isotope measurements. *Rapid Commun. Mass Spectrom.: RCM* **27**, 603–612.

Breecker D. O., Sharp Z. D. and McFadden L. D. (2009) Seasonal bias in the formation and stable isotopic composition of pedogenic carbonate in modern soils from central New Mexico, USA. *Geol. Soc. Am. Bull.* **121**, 630–640.

Carothers W. W., Adami L. H. and Rosenbauer R. J. (1988) Experimental oxygen isotope fractionation between siderite-water and phosphoric acid liberated CO_2-siderite. *Geochim. Cosmochim. Acta* **52**, 2445–2450.

Dennis K. J. and Schrag D. P. (2010) Clumped isotope thermometry of carbonatites as an indicator of diagenetic alteration. *Geochim. Cosmochim. Acta* **74**, 4110–4122.

Dennis K. J., Affek H. P., Passey B. H., Schrag D. P. and Eiler J. M. (2011) Defining an absolute reference frame for "clumped" isotope studies of CO_2. *Geochim. Cosmochim. Acta* **75**, 7117–7131.

Dennis K. J., Cochran J. K., Landman N. H. and Schrag D. P. (2013) The climate of the Late Cretaceous: new insights from the application of the carbonate clumped isotope thermometer to Western Interior Seaway macrofossil. *Earth Planet. Sci. Lett.* **362**, 51–65.

Driese S. G., Ludvigson G. A., Roberts J. A., Fowle D. A., Gonzalez L. A., Smith J. J., Vulava V. M. and McKay L. D. (2010) Micromorphology and Stable-Isotope Geochemistry of Historical Pedogenic Siderite Formed in PAH-Contaminated Alluvial Clay Soils, Tennessee, USA. *J. Sediment. Res.* **80**, 943–954.

Eagle R. A., Schauble E. A., Tripati A. K., Tütken T., Hulbert R. C. and Eiler John M. (2010) Body temperatures of modern and extinct vertebrates from ^{13}C–^{18}O bond abundances in bioapatite. *Proc. Nat. Acad. Sci. U.S.A.* **107**, 10377–10382.

Eagle R. A., Eiler J. M., Tripati A. K., Ries J. B., Freitas P. S., Hiebenthal C., Wanamaker A. D., Taviani M., Elliot M., Marenssi S., Nakamura K., Ramirez P. and Roy K. (2013) The

influence of temperature and seawater carbonate saturation state on ^{13}C–^{18}O bond ordering in bivalve mollusks. *Biogeosciences* **10**, 4591–4606.
Eiler J. M. (2011) Paleoclimate reconstruction using carbonate clumped isotope thermometry. *Quatern. Sci. Rev.* **30**, 3575–3588.
Eiler J. M. and Schauble E. (2004) $^{18}O^{13}C^{16}O$ in Earth's atmosphere. *Geochim. Cosmochim. Acta* **68**, 4767–4777.
Ghosh P., Adkins J., Affek H., Balta B., Weifu Guo., Schauble E. A., Schrag D. and Eiler John M. (2006) ^{13}C–^{18}O bonds in carbonate minerals: A new kind of paleothermometer. *Geochim. Cosmochim. Acta* **70**, 1439–1456.
Ghosh P., Eiler J., Campana S. E. and Feeney R. F. (2007) Calibration of the carbonate "clumped isotope" paleothermometer for otoliths. *Geochim. Cosmochim. Acta* **71**, 2736–2744.
Guo W., Mosenfelder J. L., Goddard W. A. and Eiler J. M. (2009) Isotopic fractionations associated with phosphoric acid digestion of carbonate minerals: Insights from first-principles theoretical modeling and clumped isotope measurements. *Geochim. Cosmochim. Acta* **73**, 7203–7225.
He B., Olack G. A. and Colman A. S. (2012) Pressure baseline correction and high-precision CO_2 clumped-isotope (Δ_{47}) measurements in bellows and micro-volume modes. *Rapid Commun. Mass Spectrom.: RCM* **26**, 2837–2853.
Henkes G. A., Passey B. H., Wanamaker A. D., Grossman E. L., Ambrose W. G. and Carroll M. L. (2013) Carbonate clumped isotope compositions of modern marine mollusk and brachiopod shells. *Geochim. Cosmochim. Acta* **106**, 307–325.
Huntington K. W., Eiler J. M., Affek H. P., Guo W., Bonifacie M., Yeung L. Y., Thiagarajan N., Passey B., Tripati A., Daëron M. and Came R. (2009) Methods and limitations of "clumped" CO_2 isotope (Δ_{47}) analysis by gas-source isotope ratio mass spectrometry. *J. Mass Spectrom.: JMS* **44**, 1318–1329.
Jimenez-Lopez C. and Romanek C. S. (2004) Precipitation kinetics and carbon isotope partitioning of inorganic siderite at 25 °C and 1 atm. *Geochim. Cosmochim. Acta* **68**, 557–571.
Kim S.-T. and O'Neil J. R. (1997) Equilibrium and nonequilibrium oxygen isotope effects in synthetic carbonates. *Geochim. Cosmochim. Acta* **61**, 3461–3475.
Ludvigson G. A., González L. A., Metzger R. A., Witzke B. J., Brenner R. L., Murillo A. P. and White T. S. (1998) Meteoric sphaerosiderite lines and their use for paleohydrology and paleoclimatology. *Geology* **26**, 1039–1042.
Ludvigson G. A., Fowle D. A., Roberts J. A., González L. A., Driese S. G., Place O. B., Villarreal M. A., Smith J. J. and Suarez M. B. (2013) Paleoclimatic applications and modern process studies of pedogenic siderite. *SEPM Spec. Publ.* **104**, 79–87.
Mortimer R. J. G. and Coleman M. L. (1997) Microbial influence on the oxygen isotopic composition of diagenetic siderite. *Geochim. Cosmochim. Acta* **61**, 1705–1711.
Passey B. H. and Henkes G. A. (2012) Carbonate clumped isotope bond reordering and geospeedometry. *Earth Planet. Sci. Lett.* **351–352**, 223–236.
Passey B. H., Levin N. E., Cerling T. E., Brown F. H. and Eiler J. M. (2010) High-temperature environments of human evolution in East Africa based on bond ordering in paleosol carbonates. *Proc. Nat. Acad. Sci. U.S.A.* **107**, 11245–11249.
Peters N. A., Huntington K. W. and Hoke G. D. (2013) Hot or not? Impact of seasonally variable soil carbonate formation on paleotemperature and O-isotope records from clumped isotope thermometry. *Earth Planet. Sci. Lett.* **361**, 208–218.
Quade J., Eiler J., Daëron M. and Achyuthan H. (2013) The clumped isotope geothermometer in soil and paleosol carbonate. *Geochim. Cosmochim. Acta* **105**, 92–107.
Rosenbaum J. and Sheppard S. M. (1986) An isotopic study of siderites, dolomites and ankerites at high temperatures. *Geochim. Cosmochim. Acta* **50**, 1147–1150.
Rosenheim B. E., Tang J. and Fernandez A. (2013) Measurement of multiply-substituted isotopologues ("clumped isotopes") of CO_2 using a 5 kV compact isotope ratio mass spectrometer: performance, reference frame, and carbonate paleothermometry. *Rapid Commun. Mass Spectrom.: RCM* **27**, 1847–1857.
Santrock J., Studley S. A. and Hayes J. M. (1985) Isotopic analyses based on the mass spectra of carbon dioxide. *Anal. Chem.* **57**, 1444–1448.
Schauble E. A., Ghosh P. and Eiler J. M. (2006) Preferential formation of ^{13}C–^{18}O bonds in carbonate minerals, estimated using first-principles lattice dynamics. *Geochim. Cosmochim. Acta* **70**, 2510–2529.
Sheldon N. D. and Tabor N. J. (2009) Quantitative paleoenvironmental and paleoclimatic reconstruction using paleosols. *Earth Sci. Rev.* **95**, 1–52.
Smith J. E., Schwarcz H. P., Risk M. J., McConnaughey T. A. and Keller N. (2000) Paleotemperatures from deep-sea corals: overcoming "vital effects". *Palaios* **15**, 25–32.
Suarez M. B., González L. A. and Ludvigson G. A. (2011) Quantification of a greenhouse hydrologic cycle from equatorial to polar latitudes: the mid-Cretaceous water bearer revisited. *Palaeogeogr. Palaeoclimatol. Palaeoecol.* **307**, 301–312.
Swart P. K., Burns S. J. and Leder J. J. (1991) Fractionation of the stable isotopes of oxygen and carbon in carbon dioxide during the reaction of calcite with phosphoric acid as a function of temperature and technique. *Chem. Geol.: Isotope Geosci. Sect.* **86**, 89–96.
Tang J., Rosenheim B. E., Dietzel M., Fernandez A. and Tripati A. K. (2013) Evaluation of kinetic effects on clumped isotope fractionation (Δ_{47}) during inorganic calcite precipitation. *Mineral. Mag.* **77**(5), 2308.
Thiagarajan N., Adkins J. and Eiler J. M. (2011) Carbonate clumped isotope thermometry of deep-sea corals and implications for vital effects. *Geochim. Cosmochim. Acta* **75**, 4416–4425.
Tripati A. K., Eagle R. A., Thiagarajan N., Gagnon A. C., Bauch H., Halloran P. R. and Eiler J. M. (2010) ^{13}C–^{18}O isotope signatures and "clumped isotope" thermometry in foraminifera and coccoliths. *Geochim. Cosmochim. Acta* **74**, 5697–5717.
Ufnar D. F., González L. A., Ludvigson G. A., Brenner R. L. and Witzke B. J. (2002) The mid-Cretaceous water bearer: isotope mass balance quantification of the Albian hydrologic cycle. *Palaeogeogr. Palaeoclimatol. Palaeoecol.* **188**, 51–71.
Ufnar D. F., González L. A., Ludvigson G. A., Brenner R. L. and Witzke B. J. (2004) Diagenetic overprinting of the sphaerosiderite palaeoclimate proxy: are records of pedogenic groundwater $\delta^{18}O$ values preserved? *Sedimentology* **51**, 127–144.
Wang Z., Schauble E. a. and Eiler J. M. (2004) Equilibrium thermodynamics of multiply substituted isotopologues of molecular gases. *Geochim. Cosmochim. Acta* **68**, 4779–4797.
Weber J. N. (1973) Deep-sea ahermatypic scleractinian corals: isotopic composition of the skeleton. *Deep Sea Res. Oceanogr. Abstr.* **20**, 901–909.
White T., González L., Ludvigson G. and Poulsen C. (2001) Middle Cretaceous greenhouse hydrologic cycle of North America. *Geology* **29**, 363a–366a.
Wiesli R., Beard B. and Johnson C. (2004) Experimental determination of Fe isotope fractionation between aqueous Fe(II), siderite and green rust in abiotic systems. *Chem. Geol.* **211**, 343–362.
Zhang C. L., Horita J., Cole D. R., Zhou J., Lovley D. R. and Phelps T. J. (2001) Temperature-dependent oxygen and carbon isotope fractionations of biogenic siderite. *Geochim. Cosmochim. Acta* **65**, 2257–2271.

Associate editor: Claire Rollion-Bard